ОБЪЕДИНЕННЫЙ
ИНСТИТУТ
ЯДЕРНЫХ
ИССЛЕДОВАНИЙ

Дубна

E4-95-201

V.O.Nesterenko[1], W.Kleinig[2], V.V.Gudkov[3], J.Kvasil[3]

SELF-CONSISTENT DESCRIPTION OF E2 AND E3 GIANT RESONANCES IN DEFORMED AND SUPERDEFORMED NUCLEI

Submitted to «Journal of Physics G»

[1]nester@thsun1.jinr.dubna.su
[2]On leave of absence from Technical University Dresden, Institute for Analysis, Dresden, Germany
[3]Department of Nuclear Physics, Charles University, V Holesovickach 2, CS-18000 Praha 8, Chekhia

1995

1 Introduction

The vibrating potential model (VPM) has been used in nuclear physics for a long time (see, for example, [1-9]). This model has an advantage to provide a self-consistent description of collective excitations without time consuming calculations. In the VPM, the residual separable forces and their strength constants are consistent with the form of the single-particle potential including all its deformation distortions. This is very important for the description of collective excitations in deformed and, especially, in superdeformed nuclei.

Up to now, numerical calculations within the VPM were mainly limited to the case of the harmonic-oscillator single-particle potential with a quadrupole deformation. In these studies, the doubly-stretched-coordinate technique was often used to transform the model equations to the form corresponding to the spherical system (see, e.g. [7-9]). However, this technique has not been developed for nuclei with other deformations, e.g., for the cases when both quadrupole and hexadecapole deformations are important. A more general version of the VPM has recently been proposed in [10-12] on the basis of the multipole expansion of a single-particle potential and ground state density. This version can be applied to systems (atomic nuclei and metal clusters) with any kind of static deformation (spherical systems are also covered) and with any single-particle-potentials (harmonic oscillator, Woods-Saxon, etc.). In this work, we present the VPM equations for atomic nuclei. In addition, the isovector interaction will be taken into account and the generalized strength function method (SFM) will be incorporated into the VPM scheme. The

SFM allows us to avoid solving of the VPM equations for every state, thus drastically simplifying the calculations. The model will be applied to the description of E2 and E3 isoscalar GR in ^{152}Dy, ^{154}Sm and ^{158}Gd with normal deformation and superdeformation ($\beta_2 = 0.6$). Nuclei ^{154}Sm and ^{158}Gd are chosen to check the VPM description of GR at normal deformation while the nucleus ^{152}Dy is taken to elucidate whether E2 and E3 GR survive at superdeformation (a superdeformed rotational band was observed in ^{152}Dy in [13]).

2 Main equations

A brief sketch of the VPM will first be presented. Following [6,10-12], we consider the simplest case of the irrotational and divergence free collective mode corresponding to the external field $f_{\lambda\mu}(\vec{r}) = r^{\lambda} Y^{d}_{\lambda\mu}(\Omega)$. Here, $Y^{d}_{\lambda\mu}(\Omega) = Y_{\lambda\mu}(\Omega) + d \cdot Y^{\dagger}_{\lambda\mu}(\Omega)$ where $Y_{\lambda\mu}(\Omega)$ is the spherical harmonic and the coefficient $d = \pm 1$ assures the hermiticity of the Hamiltonian. Requiring variations of the single-particle potential and density to be consistent (nuclear self-consistency), one can develop the VPM equations of the same form as the schematic RPA with separable forces [6,10-12]. Then, the Hamiltonian is written as

$$H = H_0 - 1/2 \sum_{\lambda\mu} \sum_{\tau\tau'} (\kappa_0^{(\lambda\mu)} + \tau\tau' \kappa_1^{(\lambda\mu)}) Q^{(\tau)}_{\lambda\mu} Q^{(\tau')}_{\lambda-\mu}, \tag{1}$$

where

$$Q^{(\tau)}_{\lambda\mu}(\vec{r}) = \vec{\nabla} V_0^{(\tau)}(\vec{r}) \cdot \vec{\nabla} f_{\lambda\mu}(\vec{r}) \tag{2}$$

and

$$(\kappa_0^{(\lambda\mu)})^{-1} = \sum_\tau \int n_0^{(\tau)}(\vec{r})\vec{\nabla}Q_{\lambda\mu}^{(\tau)}(\vec{r}) \cdot \vec{\nabla}f_{\lambda\mu}(\vec{r})d\vec{r}$$
$$= -\sum_\tau \int Q_{\lambda\mu}^{(\tau)}(\vec{r})\vec{\nabla}f_{\lambda\mu}(\vec{r}) \cdot \vec{\nabla}n_0^{(\tau)}(\vec{r})d\vec{r}. \quad (3)$$

The dispersion equation is

$$\kappa_0^{(\lambda\mu)}\kappa_1^{(\lambda\mu)}(X_{\lambda\mu t}^{(-)} - X_{\lambda\mu t}^{(+)})^2 - (1 - \kappa_0^{(\lambda\mu)}X_{\lambda\mu t})(1 - \kappa_1^{(\lambda\mu)}X_{\lambda\mu t}) = 0 \quad (4)$$

where

$$X_{\lambda\mu t} = \sum_\tau X_{\lambda\mu t}^{(\tau)} = 2\sum_\tau \sum_{kk'\in\tau} \frac{< k'|Q_{\lambda\mu}^{(\tau)}|k >^2 u_{kk'}^2\epsilon_{kk'}}{\epsilon_{kk'}^2 - \omega_{\lambda\mu t}^2}. \quad (5)$$

Eqs. (2)-(3) determine the self-consistent residual forces and the inverse strength constant of these forces in the isoscalar case. It is seen that in the VPM the residual forces (2) are consistent with the form of the single-particle potential $V_0^{(\tau)}(\vec{r})$ and the nuclear self-consistency provides the expression for the strength constant $\kappa_0^{(\lambda\mu)}$. In (1), H_0 includes the central potential $V_0^{(\tau)}(\vec{r})$, the spin-orbital interaction and pairing; $\kappa_0^{(\lambda\mu)}$ and $\kappa_1^{(\lambda\mu)}$ are the strength constants of the isoscalar and isovector residual forces; τ is equal to -1 and +1 for neutron and proton systems, respectively. In (2) and (3), $n_0^{(\tau)}(\vec{r}) = \sum_k | \mid k > |^2$ is a neutron (proton) ground state density with $| k >$ being a wave function of a single-particle state k. In (5), $\epsilon_{kk'} = \epsilon_k + \epsilon_{k'}$, ϵ_k is the one-quasiparticle energy, $u_{kk'} = u_k v_{k'} + u_{k'} v_k$, u_k and v_k are the Bogoliubov transformation coefficients, $\omega_{\lambda\mu t}$ is the root of equation (4). Since this paper is mainly devoted to the description of isoscalar GR, the isovector forces are treated in a simplified manner, i.e., without the self-consistency. They are taken of the same form as the isoscalar forces, and their strength constants are calculated as

$\kappa_1^{(\lambda\mu)} = \alpha_\lambda \kappa_0^{(\lambda\mu)}$ where the coefficient α_λ is adjusted so as to reproduce the experimental excitation energy of the isovector $E\lambda$ GR. Following the experimental systematics for isovector GR, $\omega_{exp}^{\lambda=2} = 120 - 130A^{-1/3}$ MeV and $\omega_{exp}^{\lambda=3} = 195A^{-1/3}$ MeV, one gets $\alpha_2 = -1.3$ and $\alpha_3 = -3.0$.

Using the multipole expansion for the single-particle potential $V_0(\vec{r}) = \sum_l \sum_{m=-l}^{l} V_{lm}(r) Y_{lm}^d(\Omega)$ and ground state density $n_0(\vec{r}) = \sum_l \sum_{m=-l}^{l} n_{lm}(r)$ $Y_{lm}^d(\Omega)$ (hereafter index τ is omitted for the sake of simplicity), one gets for the operator (2) [10-12]:

$$Q_{\lambda\mu d}(\vec{r}) = \sum_{LM} Y_{LM}(\Omega) \cdot \sum_{lm} Q_{\lambda Ll}^{\mu m d}(r) \tag{6}$$

where

$$Q_{\lambda Ll}^{\mu m d}(r) = (2\lambda+1)\sqrt{\frac{\lambda(2\lambda-1)}{\pi(2L+1)}}(C_{lm\lambda\mu}^{LM} + d(-1)^\mu C_{lm\lambda-\mu}^{LM})$$
$$\cdot [M_{\lambda Ll}^{(1)} \frac{dV_{lm}}{dr} r^{\lambda-1} - M_{\lambda Ll}^{(2)} V_{lm} r^{\lambda-2}]. \tag{7}$$

Here, $C_{lm\lambda\mu}^{LM}$ is the Clebsch-Gordan coefficient, $M_{\lambda Ll}^{(1)} = A_{\lambda Ll} - B_{\lambda Ll}$, $M_{\lambda Ll}^{(2)} = l \cdot A_{\lambda Ll} + (l+1) \cdot B_{\lambda Ll}$ and

$$A_{\lambda Ll} = \sqrt{(l+1)(2l+3)} \begin{pmatrix} l+1 & \lambda-1 & L \\ \lambda & l & 1 \end{pmatrix} \cdot C_{l+10\lambda-10}^{L0}, \tag{8}$$

$$B_{\lambda Ll} = \sqrt{l(2l-1)} \begin{pmatrix} l-1 & \lambda-1 & L \\ \lambda & l & 1 \end{pmatrix} \cdot C_{l-10\lambda-10}^{L0}. \tag{9}$$

Expressions (6)-(7) show that the coupling of the $\lambda\mu$ excitation with the spherical ($l = 0$) and deformed ($l = 2, 4, 6, ...$) parts of the single-particle potential leads to the appearance in the residual forces of the family of branches with the moments $|\lambda - l| \leq L \leq \lambda + l$ and parity $(-1)^\lambda$. It is seen that due to the self-consistency, the residual interaction includes all the deformation distortions of the single-particle potential. In the simplest case of the harmonic oscillator potential, the radial dependence of the operator (7) has a widely used form r^λ. For other single-particle potentials (Woods-Saxon, etc.), the nuclear self-consistency results in a more complicated radial dependence (see exp. (7)).

In Fig.1, the radial dependence of the main components of quadrupole and octupole residual forces in deformed and superdeformed ^{154}Sm is presented. This dependence is determined by the operator $Q^{\mu md}_{\lambda Ll}(r)$. The calculations have been performed with the Woods-Saxon potential [14] at the normal deformation ($\beta_2 = 0.29$ and $\beta_4 = 0.06$) and superdeformation ($\beta_2 = 0.6$ and $\beta_4 = 0$). Figure 1 shows that, for both $\lambda = 2$ and 3 collective modes, the deformation distortions (arising due to the nuclear self-consistency) and the spherical part of the residual forces are of the same order of magnitude. It is especially the case for the superdeformation. This means that the nuclear self-consistency is very important for the description of $E\lambda$ excitations in deformed and, especially, superdeformed nuclei.

The calculations for GR in deformed nuclei are known to be time consuming. At the same time, experimental data provide only averaged characteristics of GR, and thus we do not need a detailed description of every one-phonon state. In this case, the SFM is very useful [15]. This method allows us to obtain the averaged information about GR directly from the strength function, i.e., without solving the VPM equations for every state. According to [15], the strength function has the form

$$b_m(E\lambda\mu,\omega) = \sum_t \omega_t^m B(E\lambda\mu, gr \to \omega_t)\rho(\omega-\omega_t) \tag{10}$$

with the weight function $\rho(\omega-\omega_t) = \frac{1}{2\pi}\frac{\Delta}{(\omega-\omega_t)^2+(\Delta/2)^2}$. Here, $B(E\lambda\mu, gr \to \omega_t)$ is the reduced probability of the $E\lambda\mu$ transition from the ground state to the one-phonon state t. The quantity Δ is an averaging parameter.

Using the technique proposed in [15], we have obtained for the strength function (10) the general expression

$$b_m(E\lambda,\omega) = \frac{1}{\pi}\left(Im\left(z^m \frac{\tilde{Y}_{\lambda\mu}(z)}{Y_{\lambda\mu}(z)}\right)_{z=\omega+i\Delta/2} \right. \tag{11}$$

$$\left. +\Delta \sum_{k<k'} (p_{kk'}^{\lambda\mu})^2 u_{kk'}^2 \epsilon_{kk'}^m \left(\frac{(-1)^{m+1}}{(\omega+\epsilon_{kk'})^2+(\Delta/2)^2} + \frac{1}{(\omega-\epsilon_{kk'})^2+(\Delta/2)^2}\right)\right)$$

where

$$\tilde{Y}_{\lambda\mu}(z) = (\tilde{X}_{\lambda\mu}^{(+)}(z))^2(\kappa_0^{(\lambda\mu)} + \kappa_1^{(\lambda\mu)} - 4\kappa_0^{(\lambda\mu)}\kappa_1^{(\lambda\mu)} X_{\lambda\mu}^{(-)}(z))$$

$$+(\tilde{X}_{\lambda\mu}^{(-)}(z))^2(\kappa_0^{(\lambda\mu)} + \kappa_1^{(\lambda\mu)} - 4\kappa_0^{(\lambda\mu)}\kappa_1^{(\lambda\mu)} X_{\lambda\mu}^{(+)}(z))$$

$$+ 2(\kappa_0^{(\lambda\mu)} - \kappa_1^{(\lambda\mu)})\tilde{X}_{\lambda\mu}^{(+)}(z)\tilde{X}_{\lambda\mu}^{(-)}(z), \tag{12}$$

$$Y_{\lambda\mu}(z) = (1-\kappa_0^{(\lambda\mu)}X_{\lambda\mu}(z))(1-\kappa_1^{(\lambda\mu)}X_{\lambda\mu}(z))$$

$$-\kappa_0^{(\lambda\mu)}\kappa_1^{(\lambda\mu)}(X_{\lambda\mu}^{(-)}(z) - X_{\lambda\mu}^{(+)}(z))^2, \tag{13}$$

$$\tilde{X}_{\lambda\mu}(z) = \sum_\tau \tilde{X}_{\lambda\mu}^{(\tau)}(z) = 2\sum_\tau \sum_{kk'\in\tau} \frac{< k'|Q_{\mu}^{(\tau)}|k > p_{kk'}^{\lambda\mu} u_{kk'}^2 \epsilon_{kk'}}{\epsilon_{kk'}^2 - z^2}. \tag{14}$$

The function $X_{\lambda\mu}(z)$ has the same form as exp. (5) with changing $\omega_{\lambda\mu t}$ by the complex value z. In (14), $p_{kk'}^{\lambda\mu}$ is the single-particle matrix element for the $E\lambda\mu$ transition. Expression (11) is valid for $m = 0, 1, 2$ and 3.

The first term in (11) is the contribution of the residual interaction. If the isovector interaction is neglected, this term has a simple form with $\tilde{Y}_{\lambda\mu}(z) = \kappa_0^{(\lambda\mu)}(\tilde{X}_{\lambda\mu}(z))^2$ and $Y_{\lambda\mu}(z) = 1 - \kappa_0^{(\lambda\mu)} X_{\lambda\mu}(z)$. The second term in (11) represents the unperturbed strength function.

3 Results and discussion

The strength functions $b(E\lambda, \omega) \equiv b_1(E\lambda, \omega)$ for $\lambda = 2$ and 3 excitations are presented for ^{152}Dy, ^{154}Sm and ^{158}Gd in Figs. 2-6. The cases of normal deformation and superdeformation are considered. The normal deformations are taken from ref. [14] ($\beta_{20} = 0.29$ and $\beta_{40} = 0.06$) for ^{154}Sm and ^{158}Gd and from ref. [16] ($\beta_{20} = 0.14$ and $\beta_{40} = 0.02$) for ^{152}Dy. For all the nuclei the superdeformation is taken to be equal to $\beta_{20} = 0.6$ ($\beta_{40} = 0$). The neutron and proton pairing gaps are chosen to be $\Delta_p = 1.0$ MeV and $\Delta_n = 0.9$ MeV at normal deformation and $\Delta_p = \Delta_n = 0.3$ MeV at superdeformation [16]. A large single-particle basis is used. We take into account 123 neutron and 136 proton states in the energy range from -50 MeV to +40 MeV and more than 6500 and 8600 two-quasiparticle configurations for $\lambda = 2$ and 3 excitations, respectively. The energy-weighted sum rule $S_\lambda = \sum_i \omega_i B(E\lambda\mu, gr \to \omega_i)$ exhausts $80 - 100\%$ of the model-independent estimation $S_\lambda^{(0)} = \frac{\hbar^2 e^2}{8\pi m}\lambda(2\lambda+1)^2 Z < r^{2\lambda-2} >$. In Figs. 2-6, the strength functions are given starting with 2 MeV since the VPM does not provide an appropriate description of the low-lying collective states. The reason for the shortcoming is that pairing and spin-orbital interactions, that are very important for low-lying states, are not included into the self-consistent procedure.

Figs.2-4 show that the unperturbed E2 strength is mainly concentrated in a wide energy region with a centroid at 15 MeV (the unperturbed E2 GR). This bump corresponds to the $\Delta N = 2$ transitions (N is a principal shell quantum number) with the energy about $2\hbar\omega_0$ where $\hbar\omega_0 = 41 \cdot A^{-1/3}$ MeV is the energy distance between neighbour shells. The unperturbed E3 strength is mainly concentrated at 8 MeV (the low-energy E3 GR) and 23 MeV (the familiar E3 GR), which corresponds to the $\Delta N =$ 1 and 3 transitions with the energies $1\hbar\omega_0$ and $3\hbar\omega_0$, respectively. It should be noted that the unperturbed E2 and E3 GR are distinct at both normal deformation and superdeformation. As is seen below, the residual interaction changes considerably this picture, especially for the E3 GR.

Now let us consider this case, i.e. the E2 and E3 GR calculated with the residual interaction. As compared with [12], the present calculations have two important advantages. First, the isovector interaction is taken into account. As is seen from Figs.2-4, this interaction shifts part of the strength from the right shoulder of the GR to higher energies and thus removes the artificial widening of the isoscalar GR. So, the isovector interaction is important for a correct description of not only isovector but also isoscalar GR. The second advantage is that the present calculations use the microscopic ground state density $n_0(\vec{r}) = \sum_{k=1} | \mid k > |^2$ instead of the simplified expression $n_0(\vec{r}) = n_0/[1 + exp[r - R(\theta,\phi)/a]]$ calculated in [12] with the parameters of the Woods-Saxon potential [14]. As a result, the theoretical energies of E2 and E3 GR, being much overestimated (for 2 and 3.5 MeV, respectively) in [12], are in much better agreement with experimental data in the present calculations. Indeed, in ^{154}Sm we have obtained $\omega^{\lambda=2} = 12.5$ MeV and $\omega^{\lambda=3} = 21$ MeV as compared with the experimental values $\omega_{exp}^{\lambda=2} = 12.36$ MeV [4] and $\omega_{exp}^{\lambda=3} = 19.6$ MeV (the latter was obtained from the experimental systematics for the isoscalar E3 GR, $\omega_{exp}^{\lambda=3} = 105A^{-1/3}$ MeV). For ^{158}Gd, the agreement with experimental systematics for the isoscalar E2 and E3 GR is still better: the calculations give $\omega^{\lambda=2} = 11.9$ MeV and $\omega^{\lambda=3} = 20$ MeV as compared with the experimental values $\omega_{exp}^{\lambda=2} = 11.9$ MeV (the experimental systematics $\omega_{exp}^{\lambda=2} = 64A^{-1/3}$ MeV) and $\omega_{exp}^{\lambda=3} = 19.4$ MeV.

Figs. 2-4 show that the isoscalar E2 and E3 GR are well distinct at normal deformation. The superdeformation increases noticeably their fragmentation. The E2 GR, being stronger than the E3 GR, remains to be rather distinct at superdeformation (more in ^{154}Sm and ^{158}Gd and less in ^{152}Dy). As for the E3 GR, this resonance becomes rather vague. It practically disappears in ^{152}Dy. In this connection, one has to note that the conclusion [12] (based on the preliminary simplified calculations), on the E2 and E3 GR being indistinct at superdeformation, should be softened: it concerns mainly E3 GR in some particular nuclei.

The result that superdeformation can noticeably destroy the E2 and E3 GR seems to be realistic. It should be mentioned, nevertheless, that this result has been obtained under some approximations. First of all, the rotation and corresponding effects (an alignment, etc.) were not taken into account. Also, as has been mentioned above, we have derived the residual interaction starting with the external field $f_{\lambda\mu}(\vec{r}) = r^{\lambda}Y_{\lambda\mu}^{d}(\Omega)$ which corresponds to the electric field in the long-wave limit, i.e. to experimental probes, like photons and electrons. It is not clear, if the present results are valid for hadronic probes, like protons and alpha-particles. As is seen from Figs.2-4, the unperturbed E2 and E3 GR are rather well pronounced even at superdeformation. In principle, we cannot cast aside the chance that hadronic probes will not lead to so dramatic fragmentation of E2 and E3 GR as in the case of electric probes.

Figs. 2-4 demonstrate also some other features of the E2 and E3 GR. First, superdeformation leads to some increase in the energies of the E2 and E3 GR. Second, together with the E2 and E3 GR, the superdeformation influences the low-energy E3 GR located at the energy 5-10 MeV. This resonance is washed out less than the E2 GR but more than the E3 GR. Third, as was mentioned above, the calculated GR are more vague in ^{152}Dy than in ^{154}Sm and ^{158}Gd. This could be connected with the specific character of ^{152}Dy where the number of neutrons is rather close to the magic number. Fourth, the calculated isoscalar E2 and E3 GR exhaust approximately $15-25\%$ of the model-independent sum rule $S^{(0)}_{\lambda}$. This contribution does not noticeably change if one passes from normal deformation to superdeformation. At first sight, the contribution seems to be too small. But we should keep in mind that this is a contribution of the *isoscalar* GR to the sum rule embracing both isoscalar and isovector modes.

In Figs.5-6, the strength functions for the E2 and E3 GR in ^{152}Dy are presented for every projection μ. The cases of normal deformation and superdeformation are compared. It is seen that a large fragmentation of these resonances at superdeformation is caused by two reasons: (i) in-

Table 1: Contributions (in %) of μ-projections of E2 and E3 excitations in ^{152}Dy to the model sum rule S_λ (for the whole energy region 0-60 MeV)

	$\beta_{20} = 0.14$		$\beta_{20} = 0.60$	
μ	$\lambda = 2$	$\lambda = 3$	$\lambda = 2$	$\lambda = 2$
0	21	17	23	19
1	42	32	43	35
2	37	28	34	28
3	-	23	-	18

crease in their deformation splitting and (ii) a considerable fragmentation of the GR projections themselves. Just the second reason seems to be mainly responsible for washing out the E2 and E3 GR in superdeformed nuclei.

In Table 1, the contributions of μ-projections of E2 and E3 excitations to the model sum rule S_λ are presented for ^{152}Dy. These contributions were calculated for the whole energy interval 0-60 MeV. It is seen that the superdeformation does not change much the results. For both deformations and both resonances, the main contributions are from projections with $\mu \neq 0$. This is similar to the case of spherical nuclei where projections with $\mu \neq 0$ (embracing both $\pm\mu$ cases) give exactly twice as large contributions as the $\mu = 0$ projection. For the GR regions, the ratios between μ-contributions are nearly the same.

4 Conclusions

The extended version of the VPM is presented. Using the multipole expansion for the single-particle potential and ground state density and incorporating the strength function method into the VPM, this version provides the description of $E\lambda$ isoscalar GR in nuclei of any shape without time consuming calculations. The model proposed is rather general, does not need any adjusting parameters and can be effectively used for studying GR in different kinds of nuclei (deformed and superdeformed nuclei, , drip-line nuclei, etc.).

The importance of the nuclear self-consistency for deformed and superdeformed nuclei was demonstrated. The results obtained for E2 and E3 GR in deformed ^{154}Sm and ^{158}Gd are in good agreement with the available experimental data and systematics.

For the first time, the realistic calculations of the E2 and E3 GR in superdeformed nuclei have been performed. It was shown that at superdeformation the isoscalar E2 and E3 GR become much more fragmented and in some cases (the E3 GR in ^{152}Dy) practically disappear. Since we used the external field of the electric type, the results obtained concern the probes like photons and electrons.

Acknowledgement

V.O.N. is grateful to Prof. V.G.Soloviev, I.N. Mikhailov and S. Aberg and Drs. A.I.Vdovin and R.G.Nazmitdinov for useful discussions. V.O.N. and V.V.G are grateful for the support of the present work by INTAS (grant INTAS 93-0151).

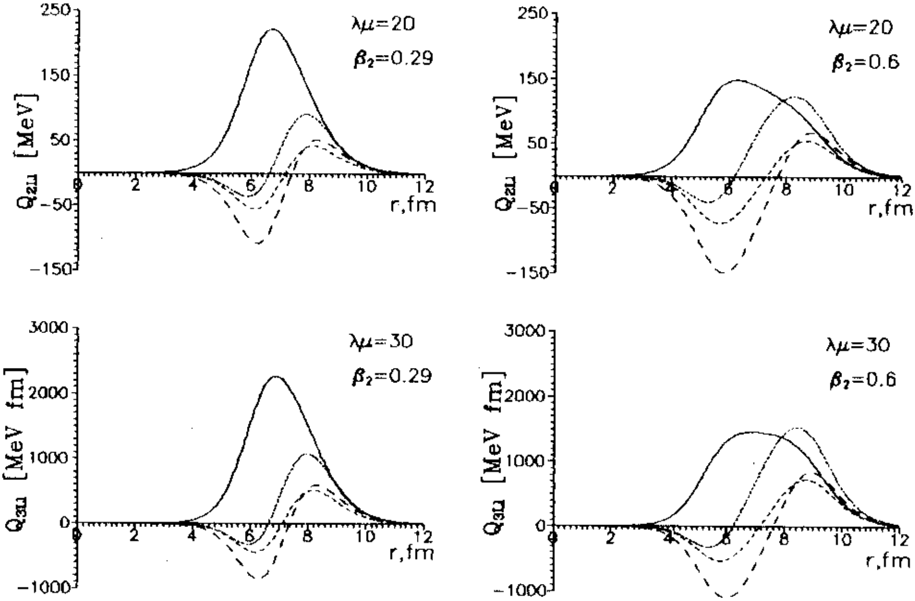

Fig.1. The radial dependence of the operator $Q^{\mu md}_{\lambda Ll}(r)$ for $\lambda\mu = 20$ (top) and $\lambda\mu = 30$ (bottom) in deformed and superdeformed ^{154}Sm. The main spherical component ($l = 0, L = 2$) and deformation distortions ($l = 2, L = 0, 2, 4$) are depicted by solid and dashed curves, respectively.

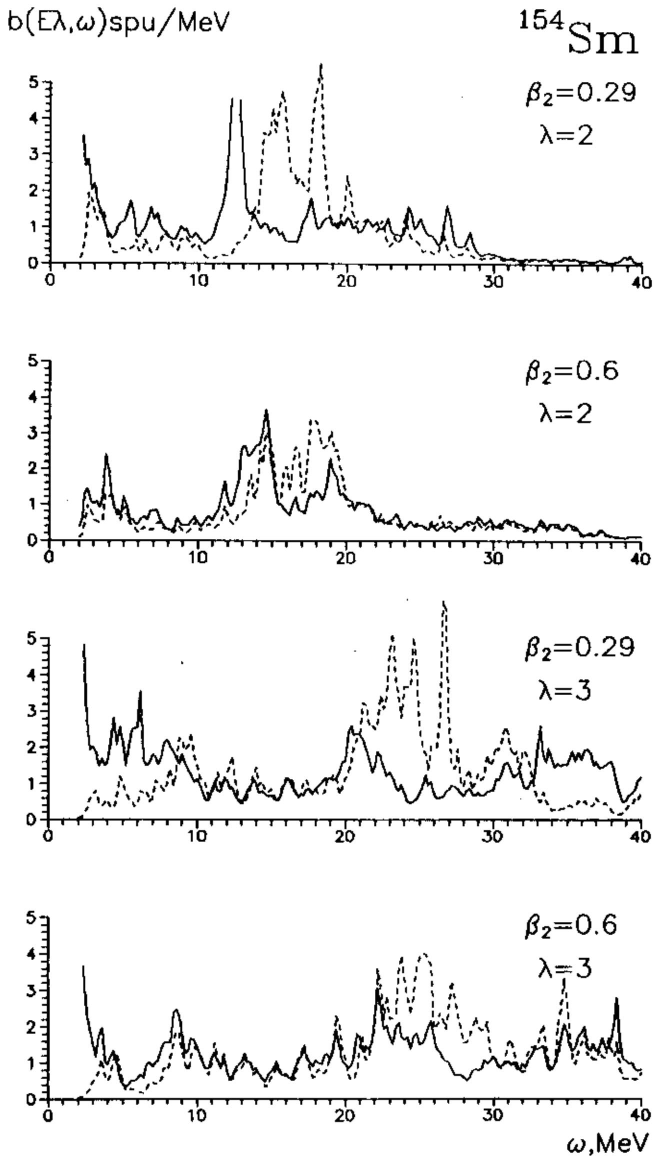

Fig.2. Strength functions $b(E2,\omega)$ and $b(E3,\omega)$ in deformed and superdeformed ^{154}Sm. The cases with (solid curve) and without (dashed curve) the residual interaction are presented. The averaging parameter Δ is equal to 0.3 MeV.

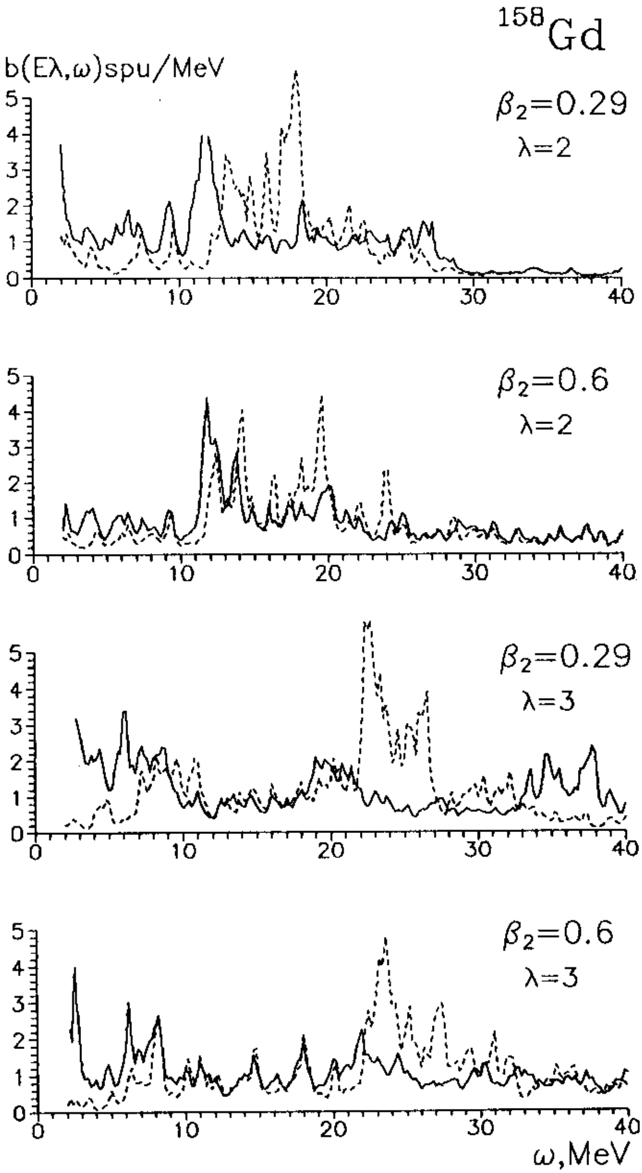

Fig.3 The same as in Fig.2 for ^{158}Gd.

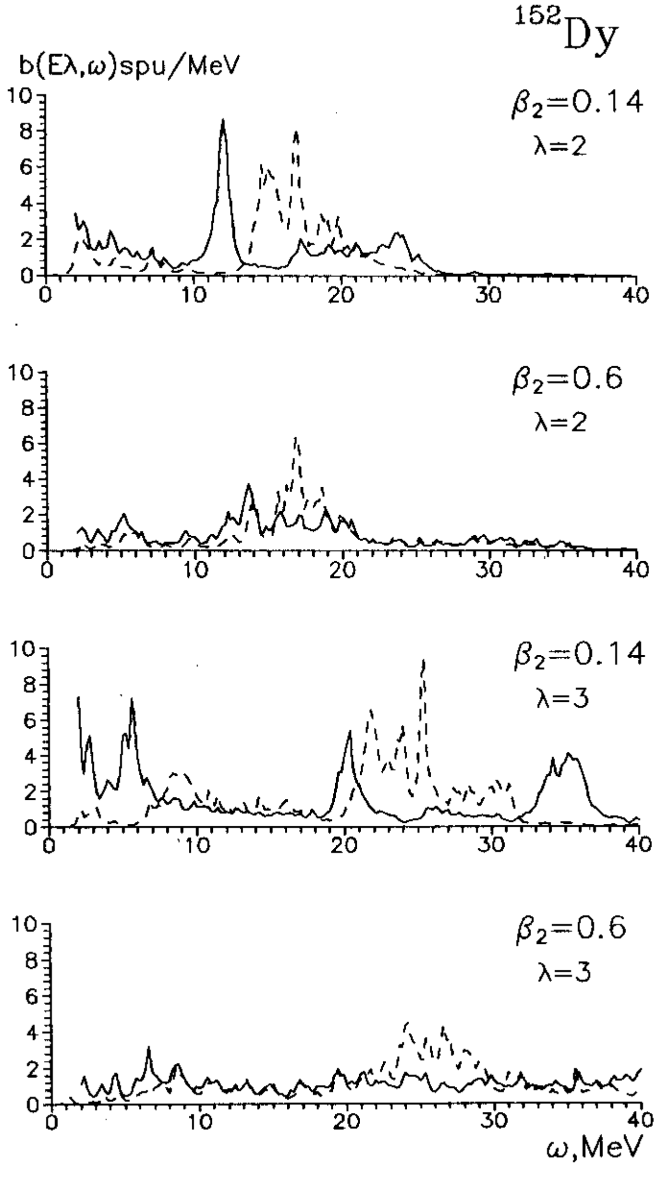

Fig.4 The same as in Fig.2 for ^{152}Dy.

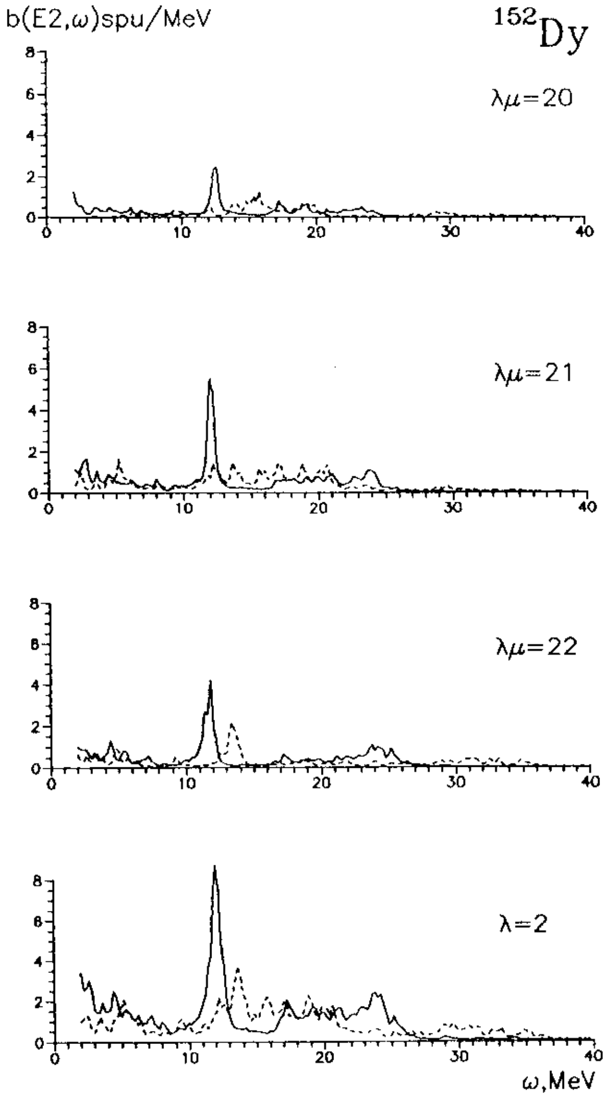

Fig.5. Strength functions for every projection μ, $b(E2\mu,\omega)$, and the total strength function $b(E2,\omega)$ in deformed (solid curve) and superdeformed (dashed curve) ^{152}Dy. The averaging parameter Δ is equal to 0.3 MeV.

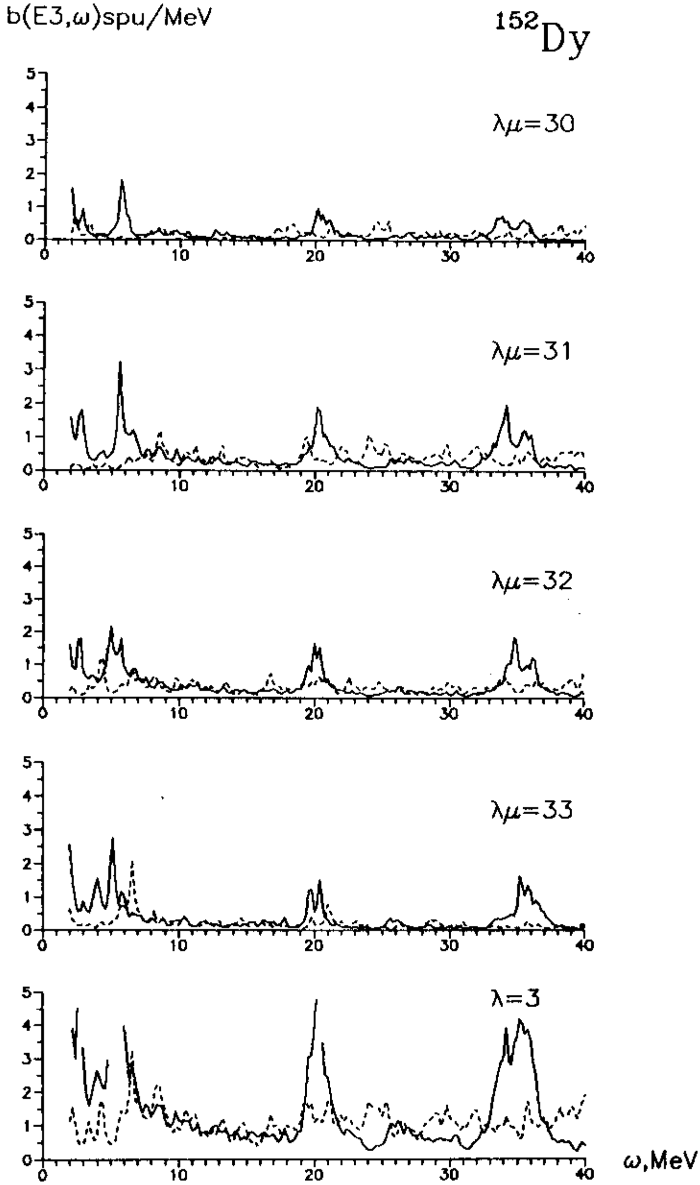

Fig.6. The same as in Fig.6 for E3 excitations.

REFERENCES

1. Rowe D J 1970 *Nuclear Collective Motion* (Methuen. London)

2. Bohr A and B.R.Mottelson B R 1975 *Nuclear Structure* v.2 (Benjamin, New-York)

3. Hamamoto I 1972 *Phys. Scr.* **6** 266

4. Kishimoto T, Moss J M, Youngblood D H, Bronson J D, Rozsa C M, Brown D R and Bacher A D (1975) *Phys. Rev. Let.* **35** 552

5. Suzuki T and Rowe D J (1977) *Nucl. Phys.* A**289** 461

6. Lipparini E and Stringari S (1981) *Nucl. Phys. A* **371** 430

7. Sakamoto H and Kishimoto T (1989) *Nucl. Phys.* A**501** 205

8. Aberg S (1985) *Phys. Lett.* B**157** 9

9. Mizutory S, Nakatsukasa T, Arita K, Shimizu Y R and Matsuyanagi K (1993) *Nucl. Phys.* A**557** 125

10. Nesterenko V O (1993) *Preprint JINR* E4-93-338, Dubna

11. Nesterenko V O, Kleinig W and Shirikova N Yu (1994) *Izv.Akad.Nauk.* ser.fiz. **58** 16

12. Nesterenko V O and Kleinig W (1995) *Phys. Scr.*, in press

13. Twin P J et al (1986) *Phys.Rev.Lett.* **57** 811

14. Gareev F A et al (1973) *Part. Nucl.* **4** 357

15. Malov L A, Nesterenko V O and Soloviev V G (1977) *Teor. Mat. Fiz.* **32** 134

16. Hamamoto I and Nazarewicz W (1992) *Phys.Let.* B**297** 25

Received by Publishing Department on April 27, 1995.